Assessment of Spatial Order in Dried Latexes by Small-Angle X-ray Scattering

N. Dingenouts and M. Ballauff*

Polymer-Institut, Universität Karlsruhe, Kaiserstrasse 12, 76128 Karlsruhe, Germany

Received April 29, 1998; Revised Manuscript Received August 11, 1998

ABSTRACT: The spatial order present in a dried latex consisting of poly(styrene) (PS) particles (diameter: 106 nm) is investigated by small-angle X-ray scattering (SAXS). The process of drying is conducted below the glass transition temperature of PS to avoid deformation of the particles when going from the concentrated latex to a system of close-contact particles. The assessment of spatial order rests on the analysis of the structure factor $S(q)$ ($q = (4\pi/\lambda)\sin(\theta/2)$; θ = scattering angle; λ = wavelength) of the dry latex. $S(q)$ has been obtained by SAXS measurements of the particles in the dilute latex and in the dried system. Special attention is paid to the different contrast between the particles and the surrounding medium when going from the waterborne latex particles to the dry film. It is demonstrated that the system under consideration here exhibits no true long-range order but a more liquidlike short range order. The data show furthermore that the deformation of the particles during the process of drying must be small if not negligible.

Introduction

The formation of solid polymer films from latex particles is a long standing problem which has been studied by many groups up to now.[1−22] A critical survey of the current literature has been given recently by Winnik.[13] The process of film formation may be subdivided into roughly three steps:[13,16,9] In a first step the water evaporates from a concentrated latex which leads to a system of latex particles in close contact. In the second step the closely packed spheres deform which leads to a space-filling film. Aging or annealing is finally effected in the third step in which a mechanically coherent film is formed through interdiffusion of the polymer chains. It is obvious that these different stages are not well separated. In case of soft particles step one and step two will more or less occur at the same time.[20,22] Monitoring the first step therefore requires hard particles with high glass transition temperatures which sustain the capillary pressure operative at the drying of the latex (cf. the discussion of this problem in refs 18 and 23).

In most cases it has been tacitly assumed that step one leads to a well-ordered three-dimensional array of latex particles. It is evident, however, that distortions of this order achieved in the first step have a profound influence on the subsequent steps since disorder induced at this stage will heal out slowly. Atomic forces microscopy (AFM) has been shown to be highly suitable to investigate the surface of films.[9,17,18,19,24−26] AFM in combination with image analysis allows to obtain the radial distribution function of the particles at the surface.[17] Electron microscopy[8,22,27] allows to assess the degree of ordering achieved in this step and to investigate the kind of close packing assumed by the spheres.

Scattering methods as e.g. small-angle X-ray scattering (SAXS)[28] and small-angle neutron scattering (SANS)[29] or turbidimetry[30] are in principle well-suited to investigate the spatial ordering during the first steps of film formation. Although SANS has been applied to the study of film formation quite frequently,[2−6,14−16,20,21] only few studies[14,21] are devoted to a systematic analysis of particle packing by SANS. Thus, Rieger et al.[21] demonstrated that regular packing of monodisperse particles lead to distinct peaks which could by assigned to a face-centered cubic lattice structure. A SANS study of this problem employing oriented samples was conducted by Joanicot et al.[14]

Up to now, no systematic study of film formation by small-angle X-ray scattering (SAXS) has been presented. On the other hand, a number of recent publications have demonstrated that SAXS is well-suited to investigate the radial structure of latex particles.[31] A problem limiting the analysis of larger particles and structures by SAXS was the restricted range of q accessible by the conventional Kratky camera. Using a modified Kratky camera, however, it has been shown that data can be obtained in a q range much enlarged ($0.03 \leq q \leq 4$ nm^{-1}) which allows the investigation of particles up to a radius R of ca. 100 nm.[32] This q range also gives the opportunity to investigate the interaction of latex particles which makes itself felt mainly at small values of qR (cf. the discussion of this point in ref 31).

Here we give a detailed account of a SAXS investigation of the first step of film formation, namely the transition from a concentrated latex to a dry film of latex particles. The underlying question is shown schematically in Figure 1: The concentrated latex (I) may form an disordered structure (II.a) upon drying or form a structure exhibiting long-range order (II.b). The consequences of the two different structures are at hand, and a quantitative determination of the spatial structure is a great interest for an understanding of e.g. the mechanical properties of the films formed after coalescence of the particles.

To study this question in detail, a poly(styrene) (PS) latex having a high glass transition temperature has been chosen. Thus, the deformation of the particles when going from state I to state II is expected to be minimal. In consequence, all alterations of the scattering intensity during the process of drying can be used to investigate the spatial order of the spheres in the dried dispersion.

10.1021/ma980682z CCC: $15.00
Published on Web 09/30/1998

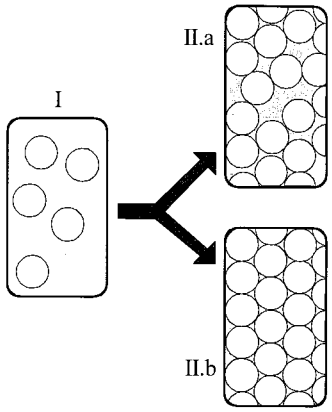

Figure 1. Scheme of the first step of film formation: transition from the concentrated latex (I) to a dry latex having different degrees of order.

The main point of the analysis to be presented here is a comparison of the scattering intensity of single particles to the scattering intensity of the dried dispersion. By a quantitative comparison of both sets of data a quantitative assessment of the spatial order present in the dry latex at stage II becomes possible. Deformations of the particles which may occur during the process of drying and their influence on the present analysis will be discussed as well.

Theory

In general, the scattering intensity of a uniform system of objects with spherical symmetry can be rendered as the product of the intensity of the isolated particles termed $I_0(q)$ and the structure factor $S(q)$[28,29]

$$I(q) = N \cdot I_0(q) \cdot S(q) \tag{1}$$

where N is the number of particles per volume and q is the magnitude of the scattering vector ($q = (4\pi/\lambda)\sin(\theta/2)$; θ = scattering angle; λ = wavelength of the Cu Kα radiation used in the experiment). The scattering intensity $I_0(q)$ of the isolated particles is given by the square of the scattering amplitude $B(q)$.[28] For spherical symmetric particles with radius R, $B(q)$ follows:

$$B(q) = 4\pi \int_0^R [\rho(r) - \rho_m] r^2 \frac{\sin(qr)}{qr} \, dr \tag{2}$$

Here $\rho(r)$ is the local electron density in the particles and ρ_m the respective value of the dispersium medium. From previous discussions[31] it is obvious that the difference between the average electron density of the particles and ρ_m determines not only the absolute magnitude of $B(q)$ but also its dependence on q. Hence, the contrast defined as the average excess electron density $\Delta\rho$ of the particles

$$\Delta\rho = 4\pi \int_0^R [\rho(r) - \rho_m] r^2 \, dr \tag{3}$$

is the decisive parameter[31] when comparing the scattering intensity of the dilute and the dried latex: In the case of PS-latex particles dispersed in water the contrast $\Delta\rho$ is low (6.4 e^-/nm^3; see ref 31); i.e., in this medium the particles are near the match point. Therefore small differences of the radial electron density $\rho(r)$ with respect to the average $\Delta\rho$ will govern $B(q)$. Thus, recent experimental studies[33,34] have demonstrated that a thin layer of a surfactant having a much higher electron density than solid PS changes the measured scattering intensity profoundly.

If, on the other hand, a powder of dry latex particles is measured by SAXS, $\rho_m \cong 0$. Here the particles have a strong contrast toward the surrounding medium air and small deviations of $\rho(r)$ from $\Delta\rho$ have no influence anymore. In this case the particles scatter in excellent approximation as homogeneous spheres. Thus, a marked influence in the scattering intensity $I_0(q)$ is expected when going from the dilute latex to the solid latex.

At high q, the scattering curves are expected to follow Porod's law[28]

$$I(q) \rightarrow N \, 2\pi\Delta\rho^2 S q^{-4} \tag{4}$$

where S is the internal surface in the system at which the electron density exhibits a discontinuity of magnitude $\Delta\rho$. For a system of known number density N and surface S eq 4 therefore allows one to determine $\Delta\rho$. It must kept in mind, however, that a thin shell affixed to particles which are nearly matched by the surrounding medium will alter the scattering intensity particularly at high q.[31] Such a shell may shift the range in which eq 4 presents a valid approximation to very large q values inaccessible by the SAXS experiment.

For polydisperse systems, the scattering intensity of a system of noninteracting particles having different sizes follows as[28]

$$I_0(q) = \sum_i N_i B_i^2(q) \tag{5}$$

where N_i denotes the number density of particles with size i. The alterations for $I_0(q)$ effected by polydispersity have been discussed at length recently.[31] The main effect of size polydispersity is a smearing of the distinct minima of $I_0(q)$ of a homogeneous sphere. On the other hand, this effect can be used to determine the standard deviation of a latex consisting of homogeneous particles.

Polydispersity has an even more pronounced effect on the structure factor as shown in detail by D'Aguanno and Klein.[35] To treat interaction in systems of polydisperse spheres, a measured structure factor $S_M(q)$ can be defined through

$$S_M(q) = \frac{I(q)}{N I_0(q)} \tag{6}$$

For a system of hard spheres, $S_M(q)$ can be calculated analytically using the Percus−Yevick theory[36] augmented by Vrij and co-workers.[37,38] For particles with known diameter and polydispersity as expressed through the standard deviation, $S_M(q)$ can be calculated as lined out by van Beurten and Vrij[38] and compared to experimental data. The measured structure factor is the central quantity since it embodies quantitative information about the range of order present in the dried latex.

Experimental Section

Materials. All chemical used herein were of analytical grade and used as received. Styrene was purified by distillation in vacuo. The poly(styrene) latex (PS) has been prepared by a conventional emulsion polymerization using potassium peroxodisulfate as initiator and sodium dodecyl sulfate (SDS) as surfactants (cf. ref 39). The concentration of the latex thus obtained was 19.6 wt %.

The latex was purified by prolonged dialysis against pure water (Milli-Ro; Millipore). Small amounts (ca. 2−4 mL) were spread out on a Petri dish to form a thin film of approximately 1 mm height and dried at ambient temperature for several days. Since the work of Winnik et al. (cf. the discussion of this point in ref 13) has demonstrated that the mode of drying may have a decisive influence on the structure of the dry latex, additional experiments were performed drying the latex film at 60 °C under normal pressure and under reduced pressure.

In all cases the drying was monitored by checking the weight of the dish. In all cases brittle pieces of dried latex were obtained. To ensure a homogeneous filling of the sample holder and an isotropic system, the pieces were ground to a powder before conducting the SAXS measurements.

All SAXS measurements were performed using a modified Kratky camera[32] in the range $0.03 \leq q \leq 4$ nm^{-1} equipped with a position-sensitive counter (Braun, München, Germany). Details of the camera and the desmearing of the raw data may be found in ref 32. In the course of these studies it could be demonstrated that the desmearing of the data obtained by the improved camera provides no difficulty.

The dilute latex was measured using a capillary holder supplied by Paar (Graz, Austria). To avoid the influence of $S(q)$ at small q, the region of smallest q values was measured at a latex concentration of 1.5 wt %. Previous investigations[31] had demonstrated that this concentration is small enough to render the effect of $S(q)$ negligible. At higher q the influence of $S(q)$ can be disregarded in excellent approximation.[31] Here it is expedient to measure $I(q)$ at much higher latex concentrations (ca. 10 wt %) and to scale the resulting data by the volume fraction. This procedure is necessary because the PS latex used in the present study has a very low contrast in water. As a consequence of this, the scattering intensity of the latex at higher q is difficult to obtain unless higher volume fractions are used for the measurements.

The sample holder used for measuring the dried powders consisted of a container of 2 mm height and 15 mm length whereas the depth (direction of the incident beam) was 1.5 mm. The sample holder was closed by windows made of thin aluminum foil (thickness: 1 μm). The entire volume of the measuring cell was calculated to 43.7 mm^3.

In this sample holder weighted amounts of the dried latex powder were filled in. The known density of solid polystyrene (1.054 g/cm^3; see ref 31) therefore allowed one to calculate the overall volume fraction of the PS spheres in the sample holder. Typical volume fractions used in the present SAXS analysis were ca. 0.43. With the size of the latex particles being known, these data served for the calculation of the number density of the particles in the sample holder.

The scattering intensity of the dried powders is much higher than the intensity measured from a dilute latex. To avoid saturation of the one-dimensional counter the scattering intensities had to be measured in two steps: The highest intensities occurring at low q were obtained by attenuating the primary beam through use of a copper foil. The attenuation amounted to typically about 0.1% of the original intensity. For these measurements the background of the sample holder was measured with the attenuation as well. The intensity at high q was obtained without attenuation, but here the low-q range was shaded off to avoid damage or saturation effects of the counter by the strong scattering. In this case the intensity of the primary beam I_0 could be measured by the moving-slit device without problems. This allowed the calculation of absolute scattering intensities. If attenuation by the copper foil was used, however, the determination of I_0 could not done with the necessary accuracy. The q range of both types of measurements overlap, however, and curves could shifted until they matched the data obtained without attenuation.

A problem which may occur at high volume fractions and contrast is multiple scattering. The scattering curve of the power (see upper curve of Figure 2a) exhibits pronounced minima and maxima which would be smeared out when multiple scattering would occur. Therefore any disturbance of the SAXS measurements by multiple scattering can be ruled out.

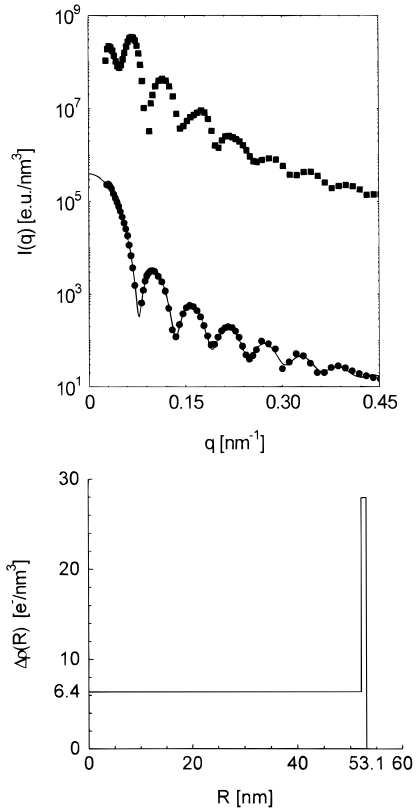

Figure 2. (a) Top: Absolute scattering intensity obtained from dilute latex particles (lower curve, filled circles; normalized to 1% volume fraction) and from dry latex powder (upper part, filled squares). The solid line in the lower part displays the fit of the radial excess electron density of the latex particles in water displayed in (b). (b) Bottom: Radial profile of the excess electron density $\rho(r)-\rho_m$. The profile has been obtained using the fit procedure described in ref 32.

Results and Discussion

As mentioned in the Introduction, the analysis presented herein rests on a quantitative comparison of $I(q)$ obtained for the dilute and for the dried latex. The assessment of order in the latex powder therefore requires the precise determination of the form factor of the latex particles. Figure 2a displays the scattering curve obtained for the latex particles dispersed in water (lower part of Figure 2a). The data have been normalized to the volume fraction of the particles. The solid line refers to a fit of the data achieved through application of the procedures described recently.[31,32] Here a core−shell structure had to be assumed having a PS core and a thin shell (thickness: 1 nm) in which $\rho(r)$ is higher by 20 e$^-$/nm^3. The corresponding radial structure $\rho(r) - \rho_m$ of the excess electron density in water is shown in Figure 2b. A similar structure was reported previously for PS latexes prepared in the presence of the surfactant SDS.[33,34] Thus, we ascribe the thin surface layer to the SDS molecules which cover the surface of the latex particles (see the discussion of this point in ref 31).

The overall number-average diameter of the spheres as determined from this fit is 106 nm. The polydispersity of the particles that results as well from this fit is small (4.8% standard deviation).

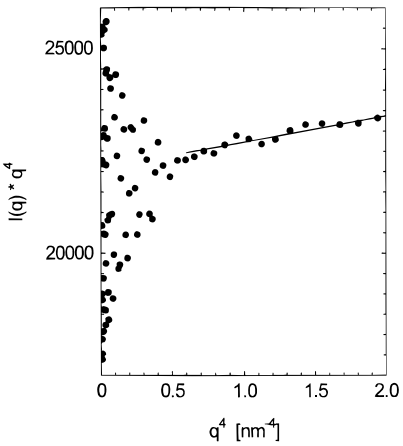

Figure 3. Porod plot (cf. eq 4) of the scattering intensities obtained from the dry latex sample. The solid line marks the q range used for the fit of the Porod constant.

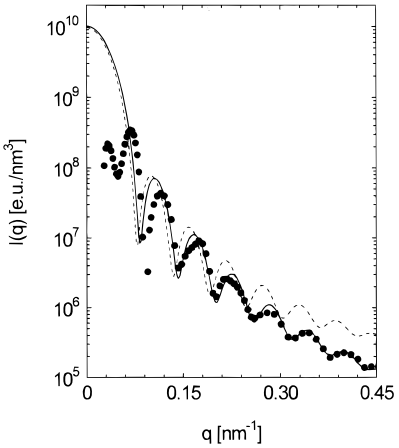

Figure 4. Comparison of the scattering intensity obtained from the dry latex sample (cf. Figure 2, lower part) with theoretical scattering functions $I_0(q)$ referring to isolated particles (cf. eq 1). The circles give the measured intensity whereas the dashed line shows $I_0(q)$ resulting from a fit of the dilute latex (see solid line of Figure 2). The solid line displays the scattering function $I_0(q)$ calculated by use of eq 3 (profile: see Figure 2b) for the PS spheres under the assumption that the particles are dispersed in vacuo ($\rho_m = 0$). See text for further explanations.

The upper part of Figure 2 refers to scattering curve obtained from the dry powder of the same latex. It could be shown that different drying procedures varying in speed of evaporation of the water did not change the scattering curves. Also, grinding coarse pieces to a powder had no measurable influence on $I(q)$. Hence, it suffices to restrict the present discussion to the data presented in Figure 2.

Since the latex has dried until constancy of weight has been reached, no water can be anymore between the particles and the contrast $\Delta\rho$ must be given by the electron density of solid polystyrene (340 e^-/nm^3). To check this point, $I(q)q^4$ at high q has been plotted against q^4 (Porod plot[28]). According to eq 4 this plot should lead to a straight line the intercept of which is given by the Porod constant (cf. eq 4). Figure 3 shows that the data taken at high follow indeed eq 4. The solid line marks the region used for the extrapolation of the Porod constant $NS\Delta\rho^2$.

The fact that the data taken at high q follow Porod's law demonstrates also that the system cannot have a true long-range order. In this case the crystalline packing of the spheres would lead to well-defined Bragg peaks in this angular region as well (cf. below).

In principle, eq 4 contains three unknowns: the number density N of the particles in the sample holder, the internal surface S, and the contrast $\Delta\rho$. As discussed in the experimental part, N can be directly obtained from the amount of latex powder in the measuring cell. Because of the uniform filling of the cell, N thus obtained is identical to the number density of the part illuminated by the primary beam.

It must be kept in mind that N calculated in this way presents an average over the entire sample holder, of course. The local number density within grains of the latex powder will be much higher and the overall volume fraction obtained from N (ca. 43 vol %) refers also to the packing of these grains in the cell (cf. below). For the evaluation according to eq 4, however, the average number density of particles in the beam must be used.

If no distortion of the particles was effected by drying, the internal surface S must be given by the surface of all particles in the scattering volume normalized to this volume, i.e., by NS. Under this assumption the contrast $\Delta\rho$ follows as 352 e^-/nm^3 whereas the theoretical value is given by 340 e^-/nm^3. In view of the various sources of error, the agreement between theory and experiment may be regarded as satisfactory. In addition to this, an electron density slightly higher than the value resulting for pure PS could be easily reconciled with the fact that the SDS molecules are still in the system. Their contribution to the electron density is small but may explain the above difference.

The data derived from the analysis of the above result immediately suggest that a strong deformation of the particles could not have taken place. Additional experiments demonstrated that a marked deformation of the particles induced by pressure lead to much smaller values of S. This is expected from the fact that fully deformed particles will fill the space entirely followed by $S = 0$.

As demonstrated above the contrast $\Delta\rho$ increases drastically when going from the dilute latex ($\Delta\rho = 6e^-/nm^3$) to the solid powder ($\Delta\rho$ = 352 e^-/nm^3). The alterations thus effected must be taken into account when calculating the measured structure factor $S_M(q)$ by application of eq 6 to the SAXS data shown in Figure 2. For this purpose $I_0(q)$ must be recalculated by use of eq 2 in which ρ_m is now set to zero. The profile $\rho(r)$, however, remains the same as the one obtained from the fit of intensities obtained from the dilute latex suspension (cf. the discussion of Figure 2). In this way the change of contrast effected through drying the latex is accounted for quantitatively.

Figure 4 demonstrates that this procedure is fully justified by the experimental data: the solid line displays the scattering intensity thus recalculated which refers to single latex spheres of 106 nm in vacuo. Possible small changes of $\rho(r)$ at the surface play no longer any role and the scattering intensity may be approximated by $I(q)$ calculated for a homogeneous PS sphere. The dashed line displays $I(q)$ obtained according to eq 2 for the same latex particles dispersed in water which has already been discussed in conjunction with Figure 2. To ensure a meaningful comparison with $I(q)$ calculated for particles in vacuo, the scattering intensities shown in Figure 2 have been multiplied so that both intensities match at $q = 0$.

At small q both scattering curve agree in first approximation as expected. At higher q, however, the

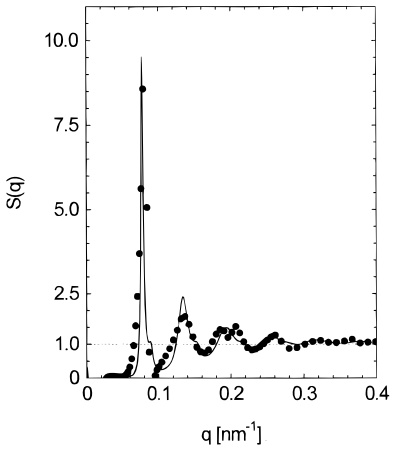

Figure 5. Comparison of the measured structure factor $S_M(q)$ calculated from experimental data according to eq 6 (circles) with the theoretical $S_M(q)$ obtained from the Percus−Yevick−Vrij model.[37,38] See text for further explanation.

scattering intensities obtained in water are considerably higher because of the radial core−shell structure. The most important feature obvious from Figure 4 is the fact that $I(q)$ calculated for spheres in vacuo matches the experimental intensities of the latex powder at higher q. While Figure 4 displays the scattering data only up to $q = 0.45$ nm^{-1}, it can be shown that the agreement of theory with experiment persists up to $q = 1.2$ nm^{-1}.

Hence, at intermediate and high q the experimental data obtained of the dried latex coincides with $I(q)$ calculated for a system of homogeneous, noninteracting spheres. Several conclusions can be drawn directly from this result: (i) The recalculated $I_0(q)$ matches the experimental data very well whereas $I_0(q)$ referring to the contrast in water would lead to erroneous data of $S_M(q)$ through application of eq 6. (ii) No strong deformation of the spheres could have taken place during the process of drying; otherwise the data at higher q could not be described anymore by the form factor of a homogeneous sphere. (iii) The dried latex powder does not exhibit true long-range order. This has been already concluded from the discussion of the Porod plot (Figure 3) because systems with infinite three-dimensional order would exhibit only Bragg peaks, of course. The data displayed in Figure 4 furthermore show that the q range in which $S_M(q)$ leads to a change of the measured intensity $I(q)$ is restricted to $q < 0.3$ nm^{-1}.

These conclusions now allow one to extract $S_M(q)$ from the experimental data through use of the intensities $I(q)$ recalculated for $\rho_m = 0$. Figure 5 displays the measured structure factor $S_M(q)$ of the dried latex obtained in this way. The effect of ordering is restricted to smaller q values indeed, beyond $q = 0.3$ nm^{-1} and $S_M(q) = 1$ within experimental error. Despite the fact that only a few points are located in the q range of the first maximum it is safe to conclude, however, that the maximum of $S_M(q)$ is considerably higher than typical values expected for the short-range order present in an equilibrium fluid.[36]

To put these considerations into a more quantitative form, the experimental data shown in Figure 5 can be compared to $S_M(q)$ calculated by the Percus−Yevick−Vrij theory (PYV)[37,38] for a system of polydisperse hard spheres. The deficiencies of the PYV theory, especially at high volume fractions, are well-known and have been discussed in detail by D'Aguanno and Klein.[35] Considering the present limits of experimental error, application of this approach appears to be justified, in particular in view of the fact that the PYV theory seems to describe subtle changes of $S_M(q)$ of polydisperse systems.[40]

The solid line gives $S_M(q)$ calculated according to PYV. The standard deviation necessary for this comparison was directly taken from the fit of the data obtained from the dilute latex (cf. the discussion of Figure 2). Hence, this quantity is directly derived from experimental data and is not used as an additional adjustable parameter. The parameters used for this fit are the volume fraction ϕ of the spheres and their diameter. The good agreement seen in Figure 5 was achieved through $\phi = 0.66$ and a diameter of 102 nm. The fit is quite sensitive to the latter parameter which gives the position of the maximum of $S_M(q)$.

Given the limitations of the PYV approach, the agreement of theory and experiment can certainly considered as satisfactory. It should be noted also that the height of the peaks of $S_M(q)$ calculated by the PYV theory depends in a sensible manner on the polydispersity of the spheres. All features of the experimental $S_M(q)$ are described quite well by the PYV result using the experimental polydispersity. This fact underscores the validity of the present fit procedure.

The volume fraction $\phi = 0.66$ taken from the fit must perhaps discussed with caution but it is certainly located between $\phi = 0.63$ characterizing random close packing and $\phi = 0.74$ which is expected for a fully ordered system of spheres. This is in qualitative accord with the height of the first maximum of $S_M(q)$ which strongly points to spatial order being more pronounced than in an equilibrium liquid.

The diameter of 102 nm is slightly smaller than the diameter derived from the fit of $I_0(q)$ (106 nm), but the difference is hardly beyond experimental uncertainty (2−4 nm). This small discrepancy may be interpreted as onset of small deformations of the spheres at the point of contact. A minor flattening of the spheres would still be compatible with the data extracted from the Porod plot and with the data displayed in Figure 4.

In the linear rendition of the data in Figure 5 the small excess intensity visible at smallest q in Figure 4 ($q \approx 0.04$ nm^{-1}) cannot be discerned anymore. We ascribe the small upturn of the measured scattering intensity in this region to a possible superstructure of the ordered regions of the particles. The existence of such a structure is evident from the fact that the volume fraction within the ordered regions is considerably higher (0.66) as compared to the overall volume fraction (0.43; see above). The upturn might therefore be identified with the final slope of larger arrays of particles. It is clear, however, that this feature of the data is beyond the q range of the present study and requires a much lower magnitude of the scattering vector than has been achieved by the equipment employed herein.

The present SAXS analysis therefore shows that drying the present latex leads to a highly ordered structure but without true long-range order. Such an order may be visualized as structure II.b depicted in Figure 1 having some slight distortions. The absence of true long-range order may easily explained by the residual but nonnegligible polydispersity of the latex

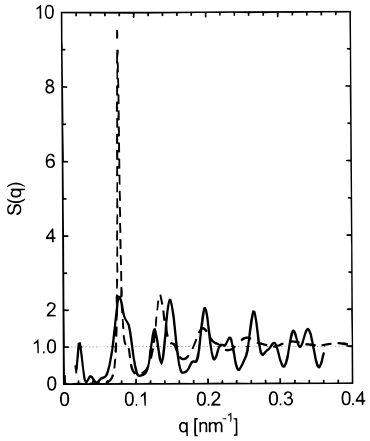

Figure 6. Comparison of the structure factor $S(q)$ deriving from the Percus−Yevick−Vrij approach (dashed line; cf. the discussion of Figure 5) and the corresponding structure factor (full line) for a system of small but fully ordered crystallites calculated according to eq 7. The crystallites consist of 108 monodisperse spheres being arranged on a perfect fcc lattice.[41]

used for this study. Additional experiments have shown that an increasing polydispersity tends to lower the order present in the dry latex drastically.[41]

As an alternative to the present description, the lack of strong reflections in $S(q)$ seen in Figure 5 may be traced back to a system of perfectly ordered but very small crystallites. To elucidate this point further, the intensity of small crystallites consisting of n monodisperse spheres having a perfect fcc structure has been calculated numerically by use of the Debye equation

$$I(q) = \sum_{i,j}^{n} B_i(q)B_j(q)\frac{\sin qd_{ij}}{qd_{ij}} \qquad (7)$$

where d_{ij} denotes the distance between sphere i and sphere j. Division of $I(q)$ thus obtained by $nB^2(q)$ gives the structure factor of the system which may directly be compared with experimental data. Details of these model calculations are given elsewhere.[41] Figure 6 gives the comparison of the PYV structure factor discussed above with the result deriving for a system of 108 spheres according to eq 7. It is immediately obvious that the present experimental results are not described by the latter model. A system of small but fully ordered crystallites is followed by broad Bragg peaks of approximately the same height. For larger crystallites the Bragg peaks become sharper and the agreement of theory and experiment becomes even worse.[41] It is therefore evident that the present system must be described in terms of a more liquidlike order as in a glassy material rather than in terms of a distorted solid consisting of many small crystallites.

The results and conclusions given here are related to a particular latex stabilized by a surfactant and characterized by a narrow size distribution. Thus, no general conclusions about the various factors influencing order in dry films can be drawn yet. The present data demonstrate unambiguously, however, that the analysis by SAXS devised herein is capable of assessing spatial order of bulk samples in a quantitative fashion. It therefore complements data taken by electron microscopy or by AFM study which reflects the order on particular surfaces.

Conclusion

An analysis of the measured structure factor $S_M(q)$ as obtained by SAXS from a dried poly(styrene) latex has been presented. SAXS is suitable to determine $S_M(q)$ if the correct contrast is applied in the course of the analysis. It has been demonstrated that this analysis allows one to assess the spatial order of the latex spheres in a quantitative fashion. In particular, the data given herein compare favorably with $S_M(q)$ calculated by the Percus−Yevick−Vrij theory[37,38] for a system of polydisperse hard spheres.

Acknowledgment. Financial support by the Bundesministerium für Bildung und Forschung, Projekt "Konzentrierte Kunststoffdispersionen", and by the Deutsche Forschungsgemeinschaft is gratefully acknowledged.

References and Notes

(1) Distler, D.; Kanig, G. *Colloid Polym. Sci.* **1978**, *256*, 1052.
(2) Hahn, K.; Ley, G.; Schuller, H.; Oberthür, R. *Colloid Polym. Sci.* **1986**, *264*, 1092.
(3) Hahn, K.; Ley, G.; Oberthür, R. *Colloid Polym. Sci.* **1988**, *266*, 631.
(4) Linné, M. A.; Klein, A.; Miller, G. A.; Sperling, L. H.; Wignall, G. D. *J. Macromol. Sci. Phys.* **1988**, *B27*, 217.
(5) Yoo, J. N.; Sperling, L. H.; Glinka, C. J. Klein, A. *Macromolecules* **1990**, *23*, 3962.
(6) Yoo, J. N.; Sperling, L. H.; Glinka, C. J.; Klein, A. *Macromolecules* **1991**, *24*, 2868.
(7) Pekan, O.; Winnik, M. A.; Croucher, M. D. *Macromolecules* **1990**, *23*, 2673.
(8) Sosnowski, S.; Li, L.; Winnik, M. A.; Clubb, B.; Shivers, R. *J. Polym. Sci., Polym. Phys.* **1994**, *32*, 2499.
(9) Juhué, D.; Wang, Y.; Lang, J.; Leung, O.; Goh, M. C.; Winnik, M. A. *J. Polym. Sci., Polym. Phys.* **1995**, *33*, 1123.
(10) Farinha, J. P. S.; Martinho, J. M. G.; Kawaguchi, S.; Yekta, A.; Winnik, M. A. *J. Phys. Chem.* **1996**, *100*, 12552.
(11) Feng, J.; Winnik, M. A.; Shivers, R. R.; Clubb, B. *Macromolecules* **1995**, *28*, 7671.
(12) Feng, J.; Winnik, M. A. *Macromolecules* **1997**, *30*, 4324.
(13) Winnik, M. A. *Curr. Opin. Colloid Interface Sci.* **1997**, *2*, 192.
(14) Joanicot, M.; Wong, K.; Marquet, J.; Chevalier, Y.; Pichot, C.; Graillat, C.; Lindner, P.; Rios, L.; Cabane, B. *Prog. Colloid Polym. Sci.* **1990**, *81*, 175.
(15) Joanicot, M.; Wong, K.; Richard, J.; Maquet, J.; Cabane, B. *Macromolecules* **1993**, *26*, 3168.
(16) Joanicot, M.; Wong, K.; Cabane, B. *Macromolecules* **1996**, *29*, 4976.
(17) Anczykowski, B.; Chi, L. F.; Fuchs, H. *Surf. Interface Anal.* **1995**, *23*, 416.
(18) Lin, F.; Meier, D. J. *Langmuir* **1995**, *11*, 2726.
(19) Lin, F.; Meier, D. J. *Langmuir* **1996**, *12*, 2774.
(20) Crowley, T. L.; Sanderson, A. R.; Morrison, J. D.; Barry, M. D.; Morton-Jones, A. J.; Rennie, A. R. *Langmuir* **1993**, *8*, 2110.
(21) Rieger, J.; Hädicke, E.; Ley, G. *Phys. Rev. Lett.* **1992**, *68*, 2782.
(22) Keddie, J. L.; Meredith, P.; Jones, R. A. L.; Donald, A. M. *Macromolecules* **1995**, *28*, 2673.
(23) Mazur, S. In *Polymer Powder Processing*; Rosenzweig, N. M., Ed.; Wiley: New York, 1995; p 157.
(24) Butt, H.-J.; Kuropka, R.; Christensen, B. *Colloid Polym. Sci.* **1994**, *272*, 1218.
(25) Butt, H.-J.; Gerharz, B. *Langmuir* **1995**, *11*, 4735.
(26) Goudy, A.; Gee, M. L.; Biggs, S.; Underwood, S. *Langmuir* **1995**, *11*, 4454.
(27) Du Chesne, A.; Gerharz, B.; Lieser, G. *Polym. Int.* **1997**, *43*, 187.
(28) Glatter, O., Kratky, O., Eds. *Small Angle X-ray Scattering*; Academic Press: London, 1982.
(29) Huggins, J. S.; Benoit, H. C. *Polymers and Neutron Scattering*; Clarendon Press: Oxford, U.K., 1994.
(30) van Tent, A.; te Nijenhuis, K. *J. Colloid Interface Sci.* **1992**, *150*, 97.
(31) Ballauff, M.; Bolze, J.; Dingenouts, N.; Hickl, P.; Pötschke, D. *Macromol. Chem. Phys.* **1996**, *197*, 3043. Dingenouts, N.; Bolze, J.; Pötschke, D.; Ballauff, M. *Adv. Polym. Sci.* 1998, in press.

(32) Dingenouts, N.; Ballauff, M. *Acta Polym.* **1998**, *49*, 178.
(33) Bolze, J.; Hörner, K. D.; Ballauff, M. *Langmuir* **1996**, *12*, 2906.
(34) Bolze, J.; Hörner, K. D.; Ballauff, M. *Colloid Polym. Sci.* **1996**, *274*, 1099.
(35) D'Aguanno, B.; Klein, R. *J. Chem. Soc., Faraday Trans.* **1991**, *87*, 379.
(36) Hansen, J. P.; McDonald, I. R. *Theory of Simple Liquids*, 2nd ed.; Academic Press: London, 1986.
(37) Vrij, A. *J. Chem. Phys.* **1979**, *71*, 3267.
(38) van Beurten, P.; Vrij, A. *J. Chem. Phys.* **1981**, *74*, 2744.
(39) Weiss, A.; Pötschke, D.; Ballauff, M. *Acta Polym.* **1996**, *47*, 333.
(40) Frenkel, D.; DeKruif, C. G.; Vos, R. J.; Vrij, A. *J. Chem. Phys.* **1986**, *84*, 4625.
(41) Dingenouts, N.; Ballauff, M. Manuscript in preparation.

MA980682Z